Cluster formation in device-to-device (D2D) communications to ensure quality of service & minimize cluster head power consumptions

Ikechukwu Harrison Ezeh

Harrison.Ezeh@futo.edu.ng

Federal University of Technology

Isaac A. Ezenugu

Imo State University

Victor N. Okorogu

Nnamdi Azikiwe University

Tochi C. Ewunonu

Federal University of Technology

Research Article

Keywords: D2D Communication, Self Organizing Map, Clustering, Power Consumption

Posted Date: May 6th, 2024

DOI: https://doi.org/10.21203/rs.3.rs-4306089/v1

Additional Declarations: No competing interests reported.

Cluster formation in device-to-device (D2D) communications to ensure quality of service & minimize cluster head power consumptions

Ezeh Ikechukwu H.[1], Ezenugu Isaac A.[2], Okorogu Victor N.[3], Ewunonu Tochi C.[4]
[1,4]*Department of Cyber Security, Federal University of Technology, Owerri, Imo State, Nigeria.*
[2]*Department of Electronic and Electrical Engineering, Imo State University, Imo State, Nigeria*
[3]*Department of Electronic and Computer Engineering, Nnamdi Azikiwe University, Awka, Anambra State, Nigeria*

Corresponding Author: ikeharris2@yahoo.com; Harrison.Ezeh@futo.edu.ng;

ORCID: 0000-0003-3856-6301

Abstract

The research proposed a clustering formation approach that ensures that the chosen cluster head (CH) in D2D communication consumes minimal energy and that the cluster members (CMs) are offered good quality of service. In addition, the study investigated various factors influencing power consumptions of User Equipment (UE) in Device to Device (D2D) Communication. Network and geographic data of the UE were collected within 200m diameter (100m radius) around the chosen base station (BS). A term Hardware Sensing Factor (a weighting factor) was formulated from the collected network data. The HSF and the distance between the UE and the base station were utilized as input data to Self Organizing Map (SOM), an unsupervised machine learning algorithm, to form clusters of the UE. A UE with highest value of HSF and minimal distance to the BS is chosen as the Cluster Head (CH) for each cluster. It was shown that the power consumption of the UE increases as the signal attenuation (which depends on distance) increases. In addition, for every transmission/reception between the Cluster Member (CM) and the BS through the CH, the CH consumes about 2.5% more than the CM. Also, in addition to the effects of signal attenuation, the power consumption of the CH is largely dependent on the number of CMs associated with the CH. Furthermore, it is more energy efficient for the CMs to communicate with the CH than communicate with the BS, especially for edge cell UE.

Key Words: *D2D Communication, Self Organizing Map, Clustering, Power Consumption*

1. Introduction

Device to device (D2D) communication enables proximate devices to have direct communication with or without the involvement of the base station (BS). It was first introduced

in 3rd Generation Partnership Project (3GPP) Long Term Evolution (LTE) Release 12 specification and had been integrated in 4G and 5G networks. D2D helps to reduce traffic intensity, latency, saves resources such as power and bandwidth, and assists in offloading traffics from the main network. During emergency situation or in the absence of base station, D2D enables the proximate devices to communicate directly and shares necessary information such as video, text and voice messages [1, 2, 3].

But the effectiveness of D2D cooperation is largely dependent on key decision processes such as cluster formation, mode selection, resource allocation and management of mobility [4]. It was further pointed out by [3] that clusters of User Equipment (UE) should be formed to allow efficient service utilization. The formation of clusters enables large networks to be divided into groups of neighbouring devices, thus allowing optimization of networks, and enhancement of social trusts, relationships and interactions. Recent works on 5G indicated that formation of clusters helps to reduce network traffics. It also enables better efficiency of energy and spectrum [5, 6, 7].

When clusters are formed, a device is chosen as the cluster head (CH) in each cluster. The CH coordinates inter- and/or intra cluster communications as well as the activities of the cluster members (CMs). The CH most often functions as a relay to forward data from the CMs to the base station (BS). In this way, the CH assists the CMs at the cell edge or CMs that have poor channel conditions to communicate with the base station. Thus, link failure is prevented and network coverage is extended [8, 9, 2, 7]. But the CH is optimally selected, because the choice of selection of CH influences the stability and reliability of clusters formed. The CH selected determines to a great extent the Quality of Service (QoS) and session continuity [4, 3].

There are three major constraints in clustered D2D communications, namely: the mobility tendency of the CH, the energy level/power consumption of the CH and the quality of service offered by the CH to the associated CMs. The mobility tendency of the CH and/or the energy level/power consumption of the CH greatly influence cluster stability or association/disassociation of the CMs. According to [4], in terms of mobility and energy dissipation, the device chosen as the CH must be reliable. This is to ensure session continuity. If the CH has high mobility tendency or high energy dissipation, frequent cluster disassociation and

re-clustering occur, thus, the availability or the reliability of the D2D communications is not guaranteed. In addition, since the CH coordinates the activities of the CMs as well as acts as relay between the CMs and the BS, it is required to be of good hardware status and to have optimum channel qualities.

The purpose of the research work is to propose solutions to the constraints in clustered D2D communication. The study proposed a clustering approach that ensures that the CH selected per a cluster would consume minimal energy and as well guarantees quality of service to the associated CMs. In order to achieve D2D cluster formation objectives, the study introduced the concepts of Hardware Sensing Factor (HSF). The HSF represents two factors: first, HSF is a weight reflecting the hardware status (in particular, the antenna sensitivity) of underlying circuitry and second, the network performance or the channel quality of D2D devices involved in the cluster formation. In addition, the study took into consideration the concept of selecting a CH with least distance to the base station; this ensures minimal energy consumptions of the CH. Thus, the two factor criteria adopted in the study work ensured that a UE with best channel quality and likelihood of least energy dissipation is selected to serve as the CH for each cluster.

2. Literature review of related work

Various cluster formation algorithms for D2D communications have been proposed in literatures. According to [10], cluster formation algorithms proposed for D2D communications can be grouped as: squared error-based algorithm, similarity-based, hierarchical based algorithms, density-based clustering algorithms, etc. Recently, machine learning algorithms have been applied in D2D communication and in particular to cluster D2D UEs [10, 11]. In addition to the choice of algorithm, various cluster data input and criteria had been adopted in literatures to cluster the UEs and select the appropriate CH. For instance, K-Means algorithm was adopted by [12] using the interference value as the input data and criterion to cluster the UEs. A combination of K-Means algorithm and Genetic Algorithm (GA) was proposed by [13]. LEACH and the variants were utilized and have been also adopted in literatures [14, 15].

Other approaches or criteria proposed in literatures include the use of distance metric, throughput, device mobility, social interactions/or relationship, device energy level, geographic

location, throughput and so on [16-20, 21]. The authors in [22] adopted the Chinese Restaurant Process (CRP) and its social variant (S-CRP) to model the formation of D2D clusters. The proposed scheme incorporated both social interactions and physical (distance) relationship among D2D terminals. The proposed clustering algorithm showed better performance in terms of throughput, power consumption and energy efficiency than other existing schemes that rely on only physical distance between D2D users. According to [16], regardless of approaches adopted, cluster formation algorithm should seek to satisfy a set of objectives which include: QoS satisfaction, cluster stability, load balancing and social awareness.

In addition to single and double factor criteria adopted by some authors, authors such as [23] proposed three factor criteria to form cluster and select the CH. The factors proposed by the authors are: the distance between the UEs, the social relationship between the UEs and the UEs energy level. It was shown by the authors that the inclusion of social relationship as one of the factors created social trust more than techniques that adopted only distance as the CH selection and cluster formation criterion. The study by [24] adopted the method of assigning of metric weights to some parameters to determine the choice of CH. The parameters which weights were assigned are: the mobility tendency of the CH, the received signal strength, the number of CMs to be supported by the CH, the time period a UE can serve as CH and the capability of the device. The UE with the least weight becomes the CH. The study showed that the high communication rate is achieved using this approach.

The adoption of various cluster formation metrics or criteria adopted in literatures serves specific purposes. For instance, the adoption of device mobility or energy level as clustering criteria can assist in reducing the rate of cluster disassociation and re-clustering. Similarly, the application of social relationships to cluster UEs will ensure that users' demand for resources and the social trust/or tie that exist among the uses can be identified. In addition, the utilization of UE geographic data as cluster formation criteria ensures social awareness and stability of the formed cluster. The reason is that proximate UEs are likely to have social interests, and distances between the UEs are considerably minimized. The considerable short distances existing between the UEs would reduce both the energy consumptions of the CHs as well as the CMs [16, 17].

In choosing the CH, the distance between it and the BS should be taken into consideration. The CH most often acts a relay to forward or receive data to and from the BS, therefore, the distance between it and the BS should be minimal. A high transmission distance between the CH and the BS imposes energy burden on the CH. But the distance of the CH from the BS depends on its location in a cluster as well as the position of the cluster in the cell. The mobility of devices may cause random distribution of the UEs around the BS or may cause the UEs to be concentrated far from the base station. In essence the distribution of the UEs is influenced by their mobility pattern and the separating distance between a UE and the BS influences its energy consumptions.

In this study, the influence of the separating distance (or signal attenuation) on the power consumptions of the UEs was investigated. Self Organizing Map (SOM), an unsupervised machine learning algorithm was utilized to form clusters of the UEs. The distance between the UEs and the base station together with the HSF served as data input to the algorithm and power consumptions of the UEs as a function of separating distance (or attenuation) were investigated.

3. Methods

3.1 Data Collection

Machine learning algorithms such as SOM need data to perform cluster formation. Some of these data can be collected by the UEs themselves, by the Radio Access Network (RAN) or by the core network [10]. The data used in this study were collected by the UEs. Data were collected from a 4G network located in dense urban residential area with tall trees and many rising buildings at Owerri (a city in eastern part of Nigeria).

3.2 Primary Data

The geographic coordinates of the BS were first determined. The latitude and longitude of the BS are 5.46726034 and 7.01624092 respectively. The determination of the BS coordinates was followed by the collection of the primary data of the UEs for hundred locations within 200m diameter (100m radius) of the cell. The primary data of the UE collected at each point were the geographic coordinates of the UEs (i.e. the Latitudes and Longitudes) and their network information [comprising of Reference Signal Received Power (RSRP), Received Signal Strength Indicator (RSSI), and Reference Signal Received Quality (RSRQ)]. The primary data namely the

Latitude, Longitude, RSRP, RSRQ and RSSI were collected during *walk test* (not drive test) at 100 points within 100m radius of the cell by selectively using four UEs from different manufacturers. The UEs types used are Nokia (NC12), Gionee M7 Lite (GM7), Infinix Smart 7 (IS7) and Tecno Spark 9 (TS9). Their hardware specifications are shown in table 1.

Table 1: Hardware Specifications and Types of UEs Used in the Study

UE Type	RAM	CPU	Storage	Battery	OS
NC12	2GB	Octa-core (4x1.6 GHz Cortex-A55)	64GB	3000 mAh	Android 12
GM7	2GB	Quad-core 1.25 GHz Mediatek	16GB	4000 mAh	Android 9.0
IS7	4GB	Octa-core (4x1.6 GHz Cortex)	64GB	5000 mAh	Android 12
TS9	4GB	Octa-core (4x2.3 GHz Cortex-A53)	64GB	5000mAh	Android 12

On each of the four UE brands, two network discovery and data collection application software namely LTE Discovery (version 4.42) and G-NetTrack Lite (version 17.3) were installed and were used to capture and record the primary data (Latitude, Longitude, RSRP, RSRQ and RSSI) at each point. Sample of the captured data using G-NetTrack Lite is shown in figure 1.

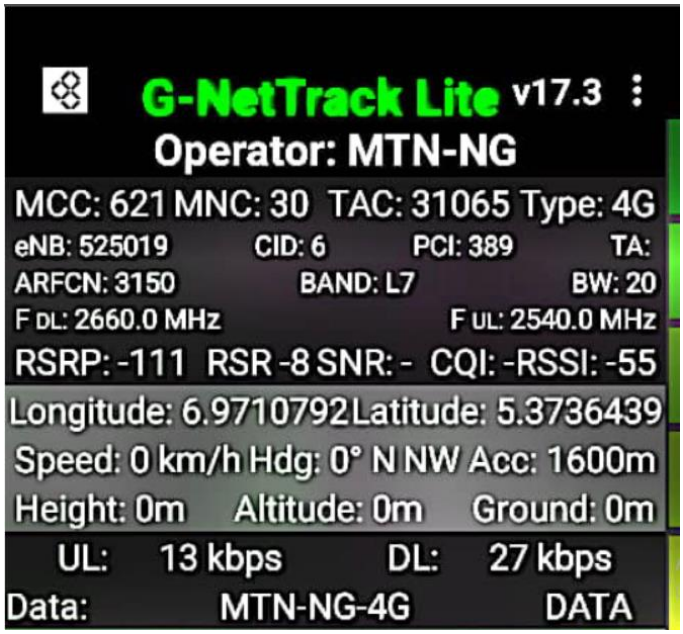

Figure 1: A Sample of Captured Primary Data using G-NetTrack Lite Application Software

3.3 Secondary Data

The captured data at each random 100 points (sample shown in figure 1) were recorded and were used to evaluate the values of the secondary data. Three secondary data were obtained. The

secondary data are: the distance (d_i) of the UE from the BS, the path loss (*PLoss*) along the link and a weighting factor termed Hardware Sensing Factor (*HSF*).

1) **Evaluation of Distance:** In this study, Haversine formula was utilized to evaluate the distance between the BS and a UE, as well as the distance between UE and another UE. The formula is represented in equation (1).

$$d = 2.R.sin^{-1}\left[\sqrt{\sin\left(\frac{\lambda_2-\lambda_1}{2}\right)^2 + sin(\frac{\varphi_2-\varphi_1}{2})^2 \,.\cos(\lambda_1)\,.\cos\,(\lambda_2)}\right] \quad (1)$$

From equation (1), if the known Latitude and Longitude of the BS are $\lambda_1$and φ_1 respectively, the captured Latitude and Longitude of a UE are λ_2 and φ_2 respectively, and R is Mean Radius of the Earth (6371 km), the separating distance *d* between the base station and the UE can be evaluated using Haversine formula of equation (1).

2) **Evaluation of the Path Loss:** If the expression in equation (1) represents the distance between a UE and the BS, it can be used to estimate the path loss (*PLoss*), since PLoss is a function of the operating frequency (*f*) and the separating distance (*d*) between the transmitter and the receiver. In this study, the modified Okumura-Hata path loss model investigated and developed by [25] was adopted to estimate the path loss between a UE and the BS, this is shown in equation (2).

$$PL_{oss} = 127.30 + 33.57 * \log d_i \quad (2)$$

where d_i is the separating distance between a UE and the BS.

3) **Evaluation of Hardware Sensing Factor (HSF):** From observations, it is evident that cellular devices from different manufactures do not report the same value of a measured network parameter, even if both are subjected to the same environment and time. For instance, while one device from a manufacturer reports a measured value of RSRP to be -87 dBm, another device from a different manufacturer located at the same spot as the former may report a value of -86 dBm. Similar observation is made even with devices from the same manufacturer of the same or different model. In addition, the measurements of a device at a location but at different time of the day differ. In this instance, the measurement is not only a function of the underlying hardware, but also dependent on the link quality.

The variations of measurement of network parameters by same device at same location but at three separate periods are depicted in figure 2, while the variations of measurement of network parameters by devices from three different vendors at the same location and within the same time interval is shown in figure 3.

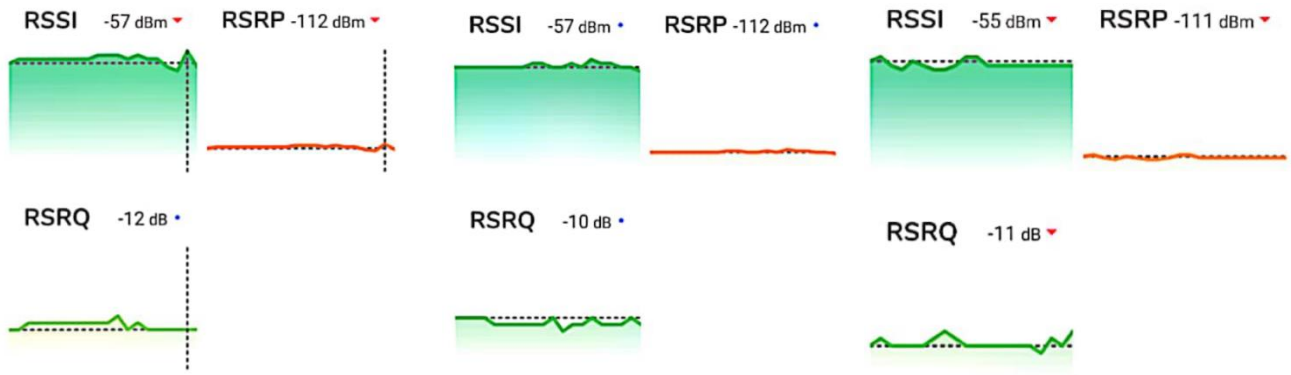

(a) (b) (c)

Figure 2: Measurement by the same UE, same Location, Different time

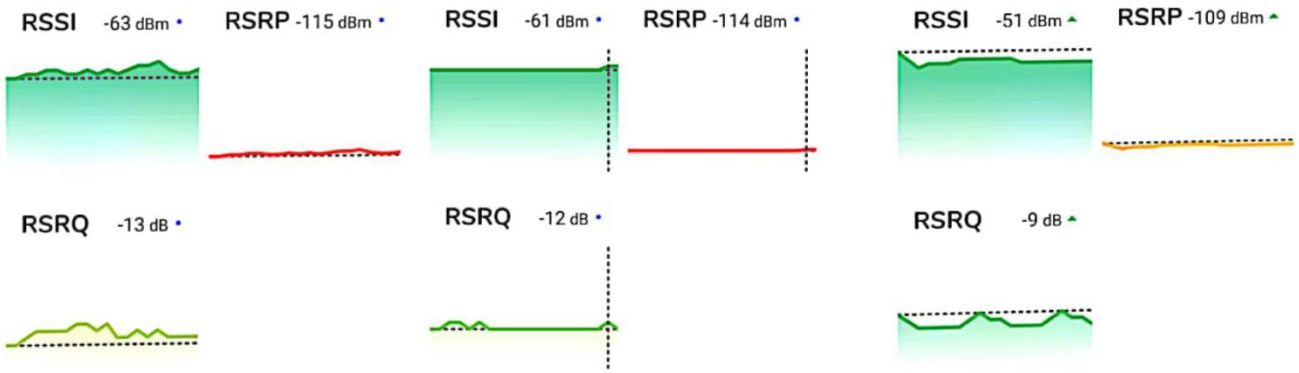

(a) (b) (c)

Figure 3: Measurement by different UEs, same Location, same time

The cause of the variations of measured network parameters by the devices of the same vendor or devices from different vendors is not far from hardware status. It has been noted in literatures that degradation of antenna sensitivity otherwise known as *desense* limits the receiver's ability to detect signals especially low-level signals. *Desense* could be attributed to both external and internal electromagnetic interferences. Internal interferences are mostly due to noise that comes from signal harmonics on patterns of printed circuit board. Such noise couples to the antenna

causing degradation in communication quality, thereby decreasing the data rata and overall communication range [26 - 28]. Thus, the value of a network quantity measured by a device is related to its hardware status. In addition, another cause of the variation is the quality of the channel or link between a device and the transmitter. The quantity or quality of a network parameter received by a device depicts the state of its link or channel condition. A device with better channel quality should have a better measured network quantity.

In this study, in addition to the use of distance between the UEs and the BS as condition or criterion for cluster formation, a weighted factor termed Hardware Sensing Factor (HSF) was also adopted. The idea is to assign numerical weights to the various ranges of the values of the reported Key Performance Indicators (KPIs) (namely RSSI, RSRP, and RSRQ). The concept of HSF takes the advantage of the facts that each KPI has ranges of values that depict the quantity or quality of the signal being received at any instance or location. Thus, HSF is a factor that reflects the hardware status of a UE as well as the overall quantity/quality of the signal receives by the device. Table 2 shows the various ranges of KPI values and the numerical weights (index factors) assigned to each range in this study.

Table 2: Weights Depicting Hardware Sensing Factor (HSF)

Description	RSRP		RSSI		RSRQ		HSF = $R_i + S_i + N_i + Qi$
	Range	RSRP Index (R_i)	Range	RSSI Index (S_i)	Range	RSRQ Index (Q_i)	
Excellent	>= -80 dBm	1.00	> -65 dBm	1.00	>= -10 dB	1.00	**3.00**
Good	-80 dBm to -90 dBm	0.75	-65 dBm to -75 dBm	0.75	-10 dB to -15 dB	0.75	**2.25**
Fair	-90 dBm to -100 dBm	0.50	-75 dBm to -85 dBm	0.50	-15 dB to -20 dB	0.50	**1.50**
Poor	<-100 dBm	0.25	< -85 dBm	0.25	< -20 dB	0.25	**0.75**

The weights assigned to each range of the values of the KPI are represented as index factor R_i, S_i, and Q_i. For any observation of these KPIs from a UE, the assigned weights are summed, and the summation gives the HSF of a UE at that observation instant. For instance,

if during a particular instant of measurement, a device reported the following KPI values: RSRP = -87 dBm, RSSI= -59 dBm, RSRQ = -11 dB. Using table 2, the corresponding index factors are: $R_i = 0.75$, $S_i = 1.00$, $Q_i = 0.75$. The HSF of the device at this observation instant is the summation of these index factors. That is, HSF = 0.75 + 1.00 + 0.75 = 2.50. From table 2, it is shown that the maximum value of HSF is 3.00, while the minimum value is 0.75. The HSF reflects the status of a UE link or channel quality as well as the status of the underlying UE circuitry. These statuses serve as a criterion to cluster the UEs and select the appropriate CH per a cluster. The higher value of HSF depicts a device with better performance, while a lower value indicates a device with lower performance. The essence of HSF is to select a UE with high hardware performance and high channel quality as the CH. The selected CH with high performance will assist the UEs whose channel conditions are poor especially those at the cell edge to relay packets to and from the BS.

Samples of UEs' geographic coordinates, the distance of the UEs from the base station, path loss, the values of the KPIs and the associated HSF are shown in table 3. The UE geographic coordinates are represented by the Latitude and Longitude columns. The distance *d* is the separating distance between the UE and the base station. The evaluated path loss along the link and other network parameters are shown in their respective columns. Additional columns namely: UE ID (containing positive integers) and UE Type (signifying the) were included to serve as UEs identifications.

Table 3 Sample Tabulation of Cluster Formation Data

UE ID	UE Type	Latitude	Longitude	Distance (m)	Path Loss	RSSI	RSRP	RSRQ	HSF
1	NC12	5.46708208	7.01618360	20.81	70.85	-69	-97	-20	1.75
-	-	-	-	-	-	-	-	-	-
22	NC12	5.46652287	7.01627270	82.08	90.85	-49	-77	-7	3.00
-	-	-	-	-	-	-	-	-	-
99	IS7	5.46719088	7.01664787	45.7	82.31	-67	-95	-10	2.00
100	IS7	5.46717114	7.01679653	62.29	86.83	-68	-96	-17	1.75

3.4 Cluster Formation Method

Self Organizing Map (SOM), an unsupervised machine learning algorithm was adopted as the clustering algorithm. SOM has the ability to determine competitively the cluster of a data set.

First, SOM determines a winner neuron, which is a neuron that has weight most similar to the data sample. This is followed by the updating of the weights of neighbor neurons, which ensures that clusters of neurons with similar weights are formed. Two functions called the learning rate $[\alpha(t)]$ and the neighborhood function $[h_{cj}(t)]$ are utilized in updating the weight vectors. The value of learning rate is between 0 & 1. While the Gaussian type of the neighborhood function is given as: $h_{uj}(t) = exp\left(-\frac{d_{uj}^2}{2\sigma^2(t)}\right)$, here, d_{uj}^2 is the distance between the winner neuron *u* and the excited neuron *j*. The radius of the neighborhood at iteration *t* is represented by the parameter σ. A simple algorithm representing SOM's algorithm is as follows:

Determine the number of cluster, represented by the number of output neuron 'n'.
Initialize the output neuron's weight vector

Set the values of the learning rate $[\alpha(t)]$ *and the neighborhood function* $[h_{cj}(t)]$
While stopping condition is not met
    For each input x
        Update the weight vector $w_j(t+1)$ *of the nearest output neuron and the neighboring neurons as:*

$$w_{ji}(t+1) = w_{ji}(t) + \alpha(t)h_{cj}(t)\left[x(t) - w_{ji}(t)\right] \quad (3)$$

End for
    Learning rate is reduced
    Neighborhood parameter is reduced
End while

The study utilized two parameters as inputs to clustering algorithm. The inputs are the distance d_i (between the BS and the UEs) and the values of HSF. The condition of selecting a CH per a cluster is based on two criteria. First, it is based on the CH with highest value of HSF. Second, it is based on the UE that has minimal distance to the base station. SOM can only cluster data set, but it is not equipped to determine a UE that should serve as the CH in a cluster. To achieve this, codes were included that would select the appropriate CH in a cluster and to determine the number of CMs in the cluster. The cluster formation algorithm is shown in table 4, while the flow chart is represented in figure 4.

Table 4: Cluster Formation using SOM Algorithm

```
Input: HSF, UE distance d_i & dev ID
// Initialize dimension for SOM
Dimension1 = 3
Dimension2 = 3
// Create the SOM dimension (in this case 3x3)
Net = selforgmap([dimnsion1 dimension2])
Train the neural network
Plot SOM topology, SOM Hits, etc
Extract data & cluster number for each data
//Sort data based on cluster data indices
UE_ID = dev_id(indices); HSF = HSF(indices), d_i = dist(indices)
Convert sorted cluster data into table variables
Initialize cluster number to 1: i = 1
While i is less than or equal to number of clusters
        Switch i
                Case i
                        Determine the UEs in cluster i
                        Determine the UE that has maximum HSF and minimum d_i
                        Set the UE that satisfied the condition above as the CH for cluster i
                        Evaluate the number of CMs in cluster i
                End
// Repeat for each i
Increment i
End
Output = {cluster number, UE_ID, CH values, number of CMs}
```

In this study, SOM hexagonal topology was adopted because it displays greater neighborhood size variance. Furthermore, 3x3 SOM architecture was utilized. This implies that there are nine (9) neurons or clusters used to cluster the data sets. In addition, it implies that out of 100 UEs,

nine (9) CHs will be selected for every cluster; the remaining 91 UEs become the CMs which are distributed in each cluster.

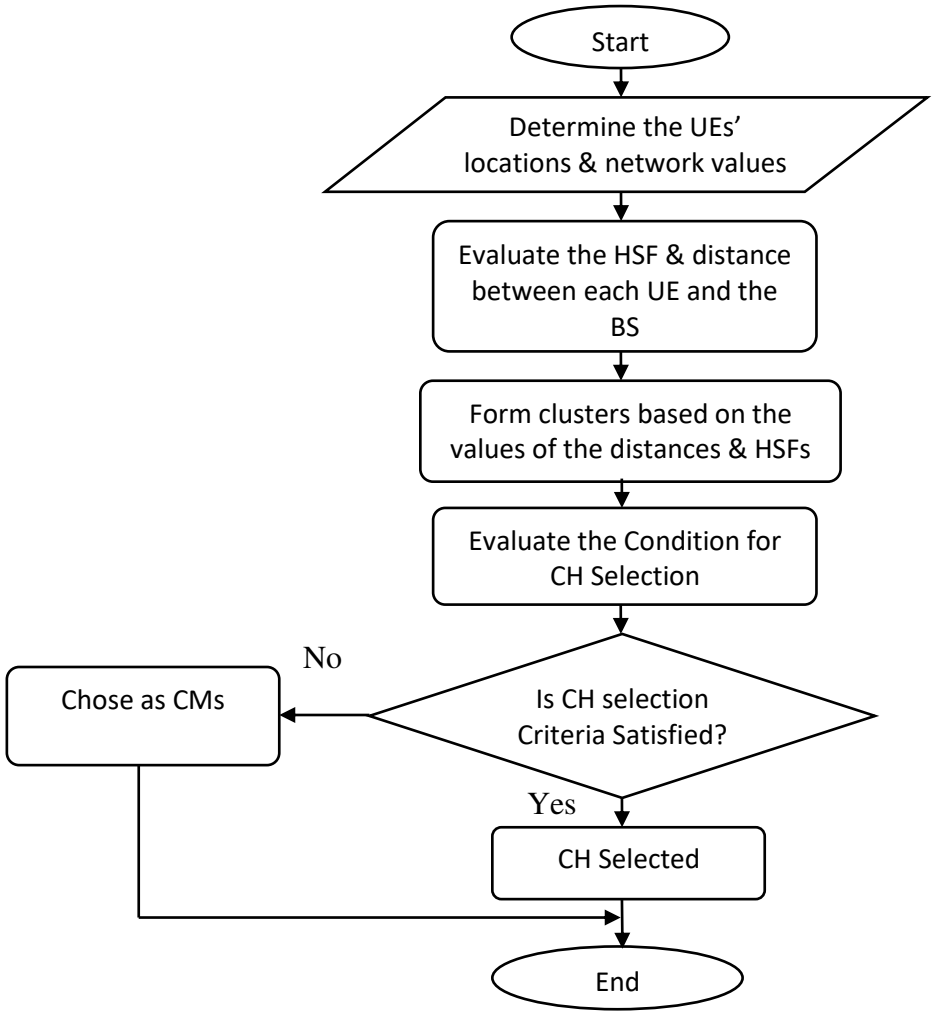

Figure 4: The Flow Chart of Cluster Formation Algorithm

3.5 Channel & Link Models

The clustering environment described a situation where the CHs connect to the BS using the conventional cellular links while the CMs communicate with one another and with the CHs using the D2D links. Thus, two distinct links were considered, namely CH-BS links and CM-CH links. Due to the existence of dual mobility of UEs over CM-CH links, various existing channel models were adapted by 3GPP. For outdoor-to-outdoor shadowing, Log normal model is specified [29]. The path loss is a random variable distributed randomly in log-domain and is given as:

$$PLoss_{LN}(dB) = PLoss_{FS} + 10nlog\left(\frac{d}{d_0}\right) + X_\sigma \qquad (4)$$

where d is the distance between the UE and BS, d_0 is the reference distance (1m to 10m for micro cell), n is the path loss exponent, X_σ is the standard deviation (σ), and $PLoss_{FS}$ is Free Space Path Loss.

Hata path loss model for urban area described by [30] was adopted for CH-BS links and is given as:

$$PLoos_{urban}(dB) = 69.55 + 26.16\,log(f) - 13.82\,log(h_{tx}) - \propto h_{rx} + [44.9 - 6.55\,log(h_{tx})]log\,(d) \quad (5)$$

where f is the frequency in MHz, d is the distance in km, the UE antenna height is given as h_{rx} in meters, and BS antenna height in meters is represented as h_{tx}. The variable $\propto h_{rx}$ has the expressions for different terrain. For large city, it is given as:

$$\propto h_{rx} = 3.2[log\,(11.75h_{rx})]^2 - 4.97;\ f > 300\text{MHz}$$
$$\propto h_{rx} = 8.29[log\,(1.54h_{rx})]^2 - 1.1;\ f \leq 300\text{MHz} \quad (6)$$

For both CM-CH and CH-BS links, Shannon wireless channel capacity C_r is represented in equation (7):

$$C_r = B.log_2(1 + \eta) \quad (7)$$

where B is the channel Bandwidth, η is the Signal to Interference and Noise Ratio (SINR). According to [31], η is expressed as:

$$\eta = {}^{P_{rx}}/_{N_oB} \quad (8)$$

where the noise spectral density is N_o, P_{rx} is the received power and B is the channel bandwidth. By substituting equation (8) into (7), the transmission rate becomes:

$$C_r = B.log_2(1 + {}^{P_{rx}}/_{N_oB}) \quad (9)$$

As described by [31], the linear expression of the received power of Okumura-Hata model is given as:

$$P_{rx} = P_{tx} . {}^{K}/_{d^\gamma} \quad (10)$$

In decibel, it is represented as:

$$P_{rx}(dB) = P_{tx}(dB) + 10log_{10}K - 10\gamma log_2(d) \quad (11)$$

where P_{rx} is the transmission power, d is the transmission distance, K is the constant path loss factor, and γ represents the path loss exponent. The received signal strength finds relationship with the path loss through the effective isotropic radiated power (*EIRP*). The expression that shows this relationship is described by [32] and is shown in equation (12):

$$P_{Loss}(dB) = EIRP - P_r(dBm) \quad (12)$$

here P_r represents the received power in (dBm). Thus, the Received Signal Strength Indicator (RSSI) could be substituted for P_r and the expression becomes:

$$EIRP = P_{Loss}(dB) + RSSI(dBm) \quad (13)$$

Equation (13) implies that the transmission power requirement (P_t) should not be less than the sum of the path loss and received power, i.e.:

$$P_t \geq P_{Loss}(dB) + RSSI(dBm) \quad (14)$$

But *RSSI* is given as: $$RSSI = RSRP + 10log_{10}(12 * N) \quad (15)$$

where *RSRP* is the Reference Signal Received Power, *N* is the number of Resource Blocks (RBs). For a bandwidth of 10 MHz, the RB is 50. The minimum value of *RSRP* as specified by 3GPP [33] is -112 dBm. Thus:

$$RSSI_{min} = RSRP_{min} + 10log_{10}(12 * N) \quad (16)$$

This shows that for bandwidth of 10 MHz, the minimum *RSSI* is -84.22 dBm. Thus equation (14) becomes:

$$P_t \geq P_{Loss}(dB) - 84.22\ (dBm) \quad (17)$$

Therefore, the transmission power requirements for CM-CH and CH-BS links are given as follows:

$$P_{tx,CM-CH} \geq PLoss_{LN}(dB) - 84.22\ (\text{dBm}) \quad (18)$$

$$P_{tx,CH-BS} \geq PLoos_{urban}(dB) - 84.22\ (\text{dBm}) \quad (19)$$

Thus, by equation (11), the received power (in dB) for CM-CH and CH-BS links is given as:

$$P_{rx,CM-CH}(dB) = P_{tx,CM-CH} + 10log_{10}K - 10\gamma log_2(d_{CM-CH}) \quad [20]$$

$$P_{rx,CH-BS}(dB) = P_{tx,CH-BS} + 10log_{10}K - 10\gamma log_2(d_{CH-BS}) \quad [21]$$

d_{CM-CH} and d_{CH-BS} are the separating distances over each link.

Hence by equation [7], the transmission rate/or capacity for each link is represented as:

$$C_{r(CM-CH)} = B.log_2\left(1 + {}^{\mathrm{P_{rx,CM-CH}}}/_{N_o.B}\right) \quad (22)$$

$$C_{r(CH-BS)} = B.log_2\left(1 + {}^{\mathrm{P_{rx,CH-BS}}}/_{N_o.B}\right) \quad (23)$$

3.6 Power Consumption Model

The power consumption of a UE during transmission ($P_{t,con}$) is the combined effects of transmission power (P_{tx}) and the power consumed by the UE analog and digital circuitry subsystems (P_{tc}). Therefore, ($P_{t,con}$) can be expressed as:

$$P_{t,con} = P_{tx} + P_{tc} \quad (24)$$

The term P_{tc}, is given as:

$$P_{tc} = P_{on} + P_{ta} \quad (25)$$

where the power consumed by the UE's cellular subsystems (CPU, graphic displays, etc) is represented as P_{on} and P_{ta} is the power consumed when the transmitter is active (i.e. transmitting). By substituting equation (23) into equation (22), $P_{t,con}$ becomes:

$$P_{t,con} = P_{tx} + P_{on} + P_{ta} \quad (26)$$

Using similar procedure, the equivalent received power consumption ($P_{r,con}$) is expressed as:

$$P_{r,con} = P_{rx} + P_{on} + P_{ra} \quad (27)$$

where, P_{rx} is the received power, P_{ra} is the power consumed when the receiver is active (i.e. receiving). It was noted by [34] and [35] that for a 4G LTE device, the value of P_{on} = 853mW, P_{ta} = 29.9mW, and $P_{ra} = 25.1\text{mW}$. Therefore, the total power consumed by UE when transmitting and receiving a packet is given as:

$$P_{Tot,con} = P_{t,con} + P_{r,con} \quad (28)$$

$$P_{Tot,con} = P_{on} + (P_{tx} + P_{ta}) + (P_{rx} + P_{ra}) \quad (29)$$

When the CMs communicate with the BS through the CH, the CMs transmit and receive from CH while the CH transmits and receives both from the BS and the CMs. This situation imposes energy burden on the CH. The total power consumed by a CM is given as $P_{CM,tot}$ and the total power consumed by a CH is given as $P_{CH,tot}$. The two are expressed in equations (30) and (31).

$$P_{CM,tot} = P_{on} + P_{CM,tx} + P_{CM,rx} \quad (30)$$

$$P_{CH,tot} = P_{on} + P_{CH,tx} + P_{CH,rx} \quad (31)$$

From equation (30), $P_{CM,tx} = P_{CM-CH,tx} + P_{CM-CH,ta}$ and $P_{CM,rx} = P_{CM-CH,rx} + P_{CM-CH,ra}$

Therefore, $P_{CM,tot} = P_{on} + \left(P_{CM-CH,tx} + P_{CM,ta}\right) + (P_{CM-CH,rx} + P_{CM,ra}\,)$ (32)

Similarly, from equation (31), CH transmits and receives to and from the BS and CMs, therefore,

$P_{CH,tx} = P_{CH-BS,tx} + P_{CH-CM,tx} + P_{CH,ta}$ and $P_{CH,rx} = P_{CH-BS,rx} + P_{CH-CM,rx} + P_{CH,ra}$

Hence,

$P_{CH,tot} = P_{on} + \left(P_{CH-BS,tx} + P_{CH-CM,tx} + P_{CH,ta}\,\right) + (P_{CH-BS,rx} + P_{CH-CM,rx} + P_{CH,ra})$ (33)

Thus, the total power consumed to transmit and receive data from the BS through the CH is given as:

$$P_{tot} = P_{CM,tot} + P_{CH,tot} \quad (34)$$

The energy expended by CM is given by:

$$E_{CM} = P_{CM,tot} \times ({}^{D_c}/_{R_{CM-CH}}) \quad (35)$$

Similarly, the energy expended by CH over CH-CM and CH-BS links are expressed as follows:

$$E_{CH-CM} = P_{CH,CM} \times ({}^{D_c}/_{R_{CH-CM}}) \quad (36)$$

$$E_{CH-BS} = P_{CH,BS} \times ({}^{D_c}/_{R_{CH-BS}}) \quad (37)$$

Where D_c is the packet content size, R is the rate of data transmission over the respective link.

4. Results and discussion

4.1 Cluster Formation Outputs

The values of the UEs' distances from the BS and the HSFs were employed as input data to SOM algorithm. The clustering was implemented in MATLAB® environment. The study utilized SOM 3x3 topology and hence there are nine clusters. Table 5 shows the statistics of the CHs selected for each cluster. The details of table 5 comprise the unique identity number of the CH (CH ID), the HSF value of the CH, the distance between the CH and the BS and the number of the associated CMs. The SOM clustering outputs indicating the number of UEs (both CMs and CH) per a cluster are displayed in figure 5.

Table 5: Cluster Statistics

Cluster Number.	CH ID	HSF	Distance (m)	Number of CMs
1	99	2.00	45.7	11
2	84	2.00	99.66	10
3	24	2.50	86.64	10
4	71	2.25	89.12	10
5	38	2.00	59.56	10
6	4	3.00	34.47	10
7	60	2.00	55.31	10
8	52	2.00	40.34	10
9	16	3.00	68.43	10

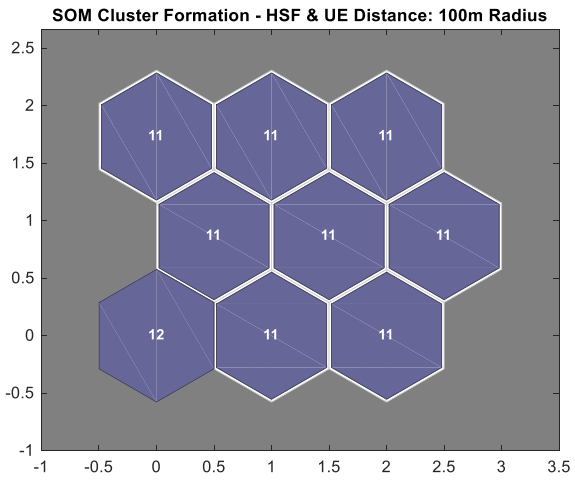

Figure 5: Outputs of Cluster Formation

It was stated previously that literatures have adopted various approaches or criteria to cluster UEs in D2D communication. In addition, it was noted that regardless of the criteria employed,

the clustering algorithm should satisfy a set of objectives, namely: quality of service offered to the CMs, the stability of the clusters formed, load balancing and social awareness. The criteria adopted to cluster the UEs in this study satisfied a greater number of this set of objectives. The combination of HSF and distance of the UE to the BS as cluster formation criteria guaranties quality of service and minimal energy consumption. With regard to QoS satisfaction, the algorithm guaranteed that a CH selected in a cluster must have the highest value of HSF. This implies that the CH channel qualities and its hardware status in particular the antenna sensitivity have the greater assigned weights and hence it is in position to offer good QoS to the associated CMs.

In addition, figure 5 and table 5 show the nine clusters formed by the algorithm and the distribution of the UEs per a cluster. It is shown that the UEs are evenly distributed among the clusters. There is a minimal difference between the number of CMs in one cluster and another cluster. The even distribution of the CMs among the cluster would guaranty that traffic loads are evenly shared among the CHs.

Furthermore, the two major factors affecting the stability of a cluster are the mobility tendency and power consumption of a CH. A CH with high mobility tendency and/or high energy consumption would lead to cluster dissolution. Though the scope of the study did not include the mobility tendency of the CH, but the use of the selection of a CH with least distance to a BS would guaranty that the power consumption of the CH is minimal, thus cluster stability is ensured.

4.2 Analysis of UEs Power Consumptions

The power consumption model established in this study pointed out that the UEs' power consumption is dependent on the transmitting distance (a factor contributing to signal attenuation). The cluster formation depicts a scenario where the CMs communicate with the BS through the CH. The CH forwards packets to and from both the BS and the CMs.

The power consumed by the UEs (CMs & CH) when connected to the BS through the CH is defined in equation (32), while the energy expended by the CMs and CH are respectively

represented by equations (33), (34) and (35). To analyze power consumptions when CMs transmit/receive data from the BS through the selected CH in the 100m radius of the study area, cluster 2 of figure 5 was utilized. Cluster 2 of figure 5 has 11 UEs (10 CMs and a CH). The locations of CMs in cluster 2 and their distances from CH are displayed in table 6 while the statistics of the selected CH are displayed in table 7.

Table 6: Locations of CMs in Cluster 2

UE ID	Latitude	Longitude	Distance (m) from CH
82	5.46714068	7.01650761	69.00
88	5.46712101	7.01654373	64.98
81	5.46710163	7.01664715	53.58
83	5.46719868	7.01694947	21.74
78	5.46715123	7.01699312	15.54
85	5.46708757	7.01633615	88.04
79	5.46710109	7.01637179	84.05
80	5.46717991	7.01647504	72.85
87	5.46712850	7.01685715	30.29
86	5.46710701	7.01641080	79.71

Table 7: Statistics of CH of Cluster 2

UE_ID	Lat	Lon	HSF	Distance from BS (m)
84	5.46712355	7.01713075	2.00	99.66

As depicted in figure 6, the power consumptions of the UEs in a cluster depends on the path loss [PL(d_i)] or signal attenuation along the links (CM-CH and CH-BS links). In addition, the power consumption of the CH depends on the signal attenuation on these links as well as on the number of the associated CMs.

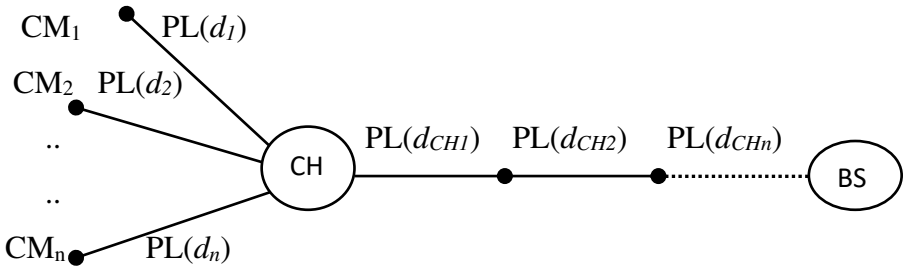

Figure 6: Factors Influencing Power Consumptions of the UEs in a Cluster

Using the mathematical models formulated previously, for CM-CH-BS links, the power consumed by only the CH to transmit/receive a packet to and from a CM and the BS is represented in Figure 7. It is observed that as the separating distance between a CM and the CH increases, the CH consumes more power during transmission/reception.

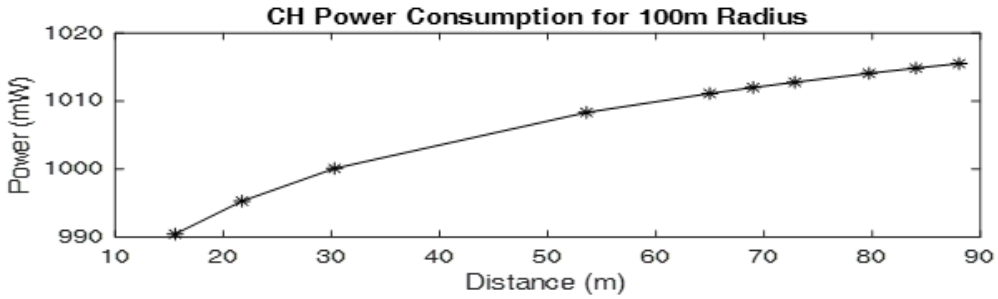

Figure 7: Power Consumption of CH over CM-CH-Bs links

Similarly, the power consumed by both the CM and CH to transmit/receive a packet over CM-CH-BS links is shown in figure 8. This is the combined power consumption of both a CM and the CH when a CM transmits and receives from BS through the CH.

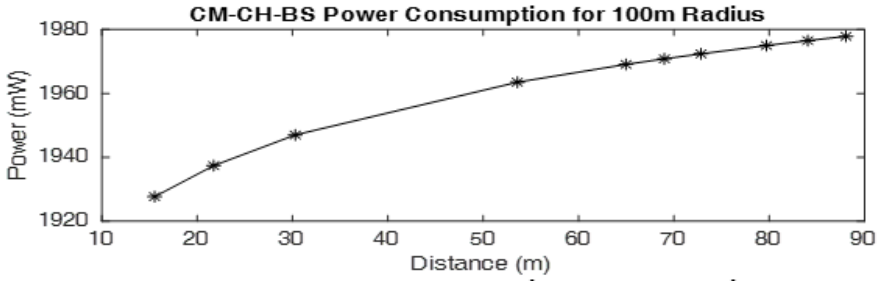

Figure 8: Power Consumption of CM & CH over CM-CH-BS links

Figure 7 represents the power consumes by only the CH over CM-CH-BS links, while figure 8 is the display of the power consume both the CMs and CH over CM-CH-BS links. Using these figures, comparison of the power consumptions of the CM and CH shows that for every transmission and reception of the CM from the base station through the CH, the CH consumes an average power of 2.5% more than the CM. The extra power consumed by the CH is due to the separating distance between the CH and the base station. Thus, the power consumption of the CH is dependent on the separating distance between the CH and CM as well as the distance between the CH and the BS.

Furthermore, when the BS is not involved, (probably, the BS is unavailable), the CMs communicates with the CH over CM-CH links. Figure 9 displays the combined power of both

the CM and the CH to transmit and receive from each other in a cluster when the base station is not involved.

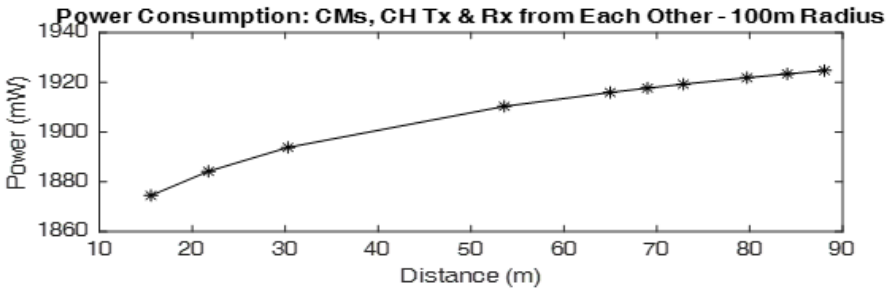

Figure 9: Power Consumptions of CM & CH in Cluster 2 over CM-CH links

A comparison of figure 8 and figure 9 indicates that the power consumption of the CMs when they communicate with the BS through the CH is greater than when they communicate with the CH. The additional energy is due to the power consumption of the CH over CH-BS link. Thus, when the UEs are farther from the base station (especially the edge cell UEs) it is more power efficient for the UEs to communicate with the CH than to communicate with the BS.

Furthermore, the UEs in cluster 1, 2, 4, 5 and 9 were used to illustrate the power consumptions of the UEs with various CH-BS distances. The distances over the CM-CH links in each cluster were determined along with the distances over the CH-BS links. The plot of the power consumption in each cluster is shown in figure 10.

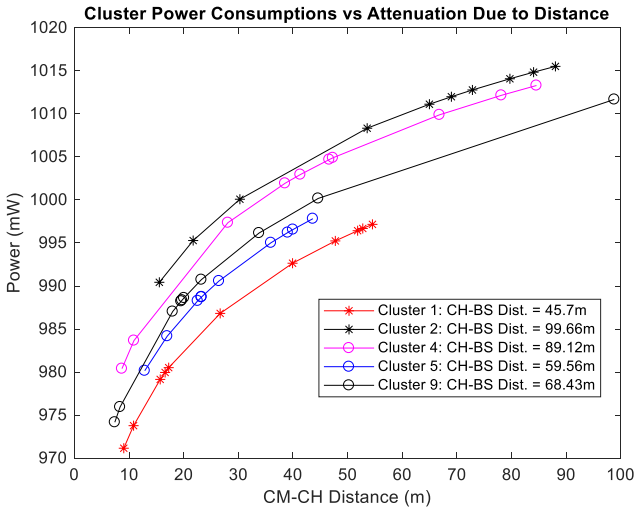

Figure 10: Cluster Power Consumptions for Various CH-BS distances

It is observed that the distance over CH-BS links contribute largely to the power consumes in a cluster. A cluster with large CH-BS distance consumes more energy than a cluster with less CH-BS distance.

In addition, figure 6 indicates that the power consumption of CH depends not only on the signal attenuation due to distance but also on the number of the associated CMs. Figure 7 is a representation of power consumption of CH in cluster 2 when the associated 10 CMs are communicating with the CH. But all the CMs may not be communicating with the CH at the same time. The power consumptions of the CH of cluster 2 when it is transmitting and receiving from 4, 5 and 7 CMs are displayed in Figure 11.

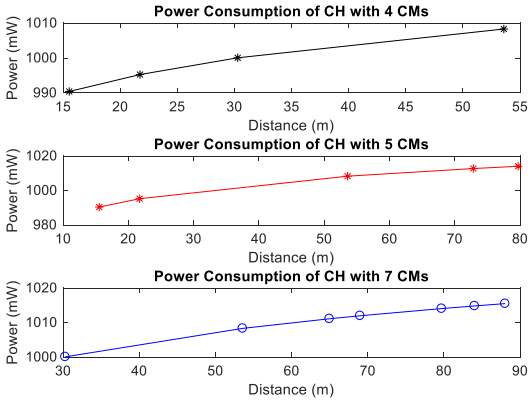

Figure 11: Power Consumption of the CH of Cluster 2 with Varying number of CMs

A comparison of figure 7 with figure 11 reveals that the power consumption of CH varies with varying number CMs. As the number of CMs with large CM-CH link distance increases, the CH power consumption increases.

5. Conclusion

The study was conducted to proffer efficient cluster formation solution that would ensure that the CH in D2D communication consumes minimal energy and that the CMs are offered good quality of service. In addition, the research investigated physical factors that affect the UE power consumptions in clustered D2D communication. The utilization and the combination of the novel concept of HSF and distance between the UE and BS as cluster input data used in this study ensures that a CH with high hardware status, good channel quality and less energy consumption is selected for each cluster. These features of the selected CH would ensure that good quality of

service is offered to the associated CMs. In addition, the power consumption of the CH is minimized and this will contribute to the reliability of D2D links. It was shown that in addition to the power consumes by the UE's underlying circuitry, the signal attenuation along the link and the number of associated CMs play a great role in its power consumption.

Table 6: Parametric Assumptions

Parameter	Assumption
Cellular Diameter	1 km
Number of UE	100
Bandwidth	10 MHz
Required transmission power, P_t	$\geq P_{Loss}(dB) + RSSI_{min}(dBm)$
Power consumed by the UE's cellular subsystem, P_{on}	853 mW
Power consumed when the transmitter is active, P_{ta}	29.9 mW
Power consumed when the receiver is active, P_{ra}	25.1 mW
Frequency	2600 MHz
Cellular link path loss model	Hata model
D2D link path loss model	Log Normal model
Path loss exponent for cellular link	3.67
Path loss exponent for D2D link	3.5
Standard deviation, σ	9
Constant path loss factor (K)	0.0070
Noise Power Spectrum Density (N_0)	-174 dBm/Hz
Packet Size	200 bytes

Acknowledgements

Except the contributory authors, no other individual or organization that required to be acknowledged for any role in the completion of the research work.

Authors' contributions

EIH and OVN did the research conceptualization, data gathering, methodology and analysis. EIA and ETC coordinated script writing, article editing, corrections and validations of results.

Funding

The research was funded by the authors.

Availability of data and materials

The data is available on request.

Declarations

Competing interests

The authors wish to declare that there is no conflict of interest.

References

1 Condoluci M, Militano L, Orsino A, Alonso-Zarate J, Araniti G (2015) LTE-Direct vs. WiFi-Direct for Machine-type communications over LTE-A systems. 2015 IEEE 26th Int. Symp on Per, Indoor and Mob Radio Commun - (PIMRC): Workshop on M2M Communications: Challenges, Solutions and Applications. 2298-2302 https://www.researchgate.net/publication/287644192_LTE-direct_vs_WiFi-direct_for_machine-type_communications_over_LTE-A_systems. Accessed May 7, 2023

2 Jameel F, Hamid Z, Jabeen F, Zeadally S, Javed MA (2018) A Survey of device-to-device communications: Research issues and challenges. IEEE Commun Surv & Tutor, *20*:2133-2168. DOI:10.1109/COMST.2018.2828120

3 Paramonov A, Hussain O, Samouylov K, Koucheryavy A, Kirichek R, Koucheryavy, Y. (2017) Clustering optimization for out-of-band D2D communications. Wirel Commun and Mob Comput. *2017*(6747052):1-11. https://doi.org/10.1155/2017/6747052.

4 Sharafeddine S. Farhat O (2018) A proactive scalable approach for reliable cluster formation in wireless networks with D2D offloading. *Ad Hoc Netw*, 77:42-53. https://www.sciencedirect.com/science/article/abs/pii/S1570870518301483?via%3Dihub Accessed August 12, 2023.

5 Wang L, Araniti G, Cao C, Wang W, Liu Y (2015) Device-to-Device users clustering based on physical and social characteristics. Inter J of Distrib Sens Netw. *2015*(165608):1-14. https://journals.sagepub.com/doi/pdf/10.1155/2015/165608. Accessed May 17, 2023.

6 Bentaleb A, Boubetra A, Harous S (2013) Survey of clustering schemes in Mobile Ad hoc networks. Commun and Netw 5:8-14. https://www.scirp.org/pdf/CN_2013071009593748.pdf. Accessed June 4, 2023.

7 Ashraf M, Yeo W.-Y, Woo M, Lee, K.-G (2016). Smart energy efficient device-to-multidevice cooperative clustering for multicasting content. Int J of Distrib Sens Netw, *2016*(3727918):1-9. https://journals.sagepub.com/doi/10.1155/2016/3727918 Accessed June 24, 2023.

8 Khatoon N, Amritanjali (2017). Mobility aware energy efficient clustering for MANET: A Bio-inspired approach with Particle Swarm Optimization. *Wireless Commun and Mob Comput*, *2017*(1903190): 1-12. http://downloads.hindawi.com/journals/wcmc/2017/1903190.pdf Accessed September 8, 2023.

9 Ishtiaq A, Ahmed S, Khan MF, Aadil F, Maqsood M, Khan S (2019) Intelligent clustering using moth flame optimizer for vehicular ad hoc networks. Inter J of Distribu Sens Netw, 15(1):1-13. https://journals.sagepub.com/doi/pdf/10.1177/1550147718824460 Accessed September 25, 2023.

10 Aslam S, Alam F, Hasan SF, Rashid MA (2021) A machine learning approach to enhance the performance of D2D-enabled clustered networks. *IEEE Access*, 9:16114-16132. https://ieeexplore.ieee.org/stamp/stamp.jsp?arnumber=9328769. Accessed January 2, 2023

11 Hashima S; ElHalawany BM; Hatano K; Wu, K; Mohamed EM (2021). Leveraging Machine-Learning for D2D Communications in 5G/Beyond 5G Networks. Electronics, 10(169):1-16. https://doi.org/10.3390/electronics10020169. Accessed February 14, 2023.

12 Huang X, Zeng M, Fan J, Fan X, Tang X (2018a) A Full Duplex D2D Clustering Resource Allocation Scheme Based on a -Means Algorithm. Wirel Commun and Mob Comput. 2018(1843083):1-8. https://www.hindawi.com/journals/wcmc/2018/1843083/. Accessed July 17, 2023.

13 Lee YH, Tseng HW, Lo CY, Jan YG, Chin LP, Song TC, Hsu HI (2012) Using Genetic Algorithm with Frequency Hopping in Device to Device Communication (D2DC) interference mitigation. 2012 IEEE Int Symp on Intell Signal Process and Commun Syst (ISPACS 2012), November 4-7, 201-206. http://tkuir.lib.tku.edu.tw/dspace/retrieve/52760/B2.6.pdf. Accessed July 12, 2023.

14 Midasala V, Bhavanam SN, Siddaiah P (2016) Performance analysis of LEACH protocol for D2D communication in LTE-advanced network. 2016 IEEE Int Conf on Comput Intell and Comput Res (ICCIC), 1-3. https://www.researchgate.net/publication/316902746_Performance_analysis_of_LEACH_protocol_for_D2D_communication_in_LTE-advanced_network. Accessed July 25, 2023.

15 Zhao Y, Liu K, Xu X, Yang H, Huang L (2019) Distributed dynamic cluster-head selection and clustering for massive IoT access in 5G networks. Appl Sci. 9(1):1-15. http://dx.doi.org/10.3390/app9010132

16 Khan MF, Yau K, Noor RM, Imran M (2020) Survey and taxonomy of clustering algorithms in 5G. J of Netw and Comput Appl. 154(102539). https://doi.org/10.1016/j.jnca.2020.102539

17 Ezeh IH, Idigo VE, Okorogu VN (2021) Clustering approaches in Device-to-Device Communications. IOSR J of Electron and Commun Eng (IOSR-JECE). 1(5):35-44.

18 Aslam S (2021). Clustering algorithm for D2D communication in next generation cellular networks. (Doctoral dissertation, Electrical Engineering, Massey University, Auckland, New Zealand). https://mro.massey.ac.nz/bitstream/handle/10179/16841/AslamPhDThesis.pdf?sequence=1&isAllowed=y. Accessed August 26, 2023.

19 Elshrkasi A, Dimyati K, Khairol ABA, Said M, F, M (2022) Enhancement of cellular networks via an improved clustering technique with D2D communication for mission-critical applications. ScienceDirect. 206, 103482 https://doi.org/10.1016/j.jnca.2022.103482.

20 Nasaruddin N, Yunida Y, Ramzi A (2022) Inter-clustering Cooperative Relay Selection Schemes for 5G Device-to-device Communication Networks. J of Inf and Commun Converg Eng, 20(3): 143-152. https://www.jicce.org/journal/view.html?pn=vol&uid=1180&vmd=Full. Accessed June 17, 2023.

21 Tolga G, Ahmet CK (2021) Clustering-based device-to-device discovery and content delivery in wireless networks. ITU J on Futur and Evolv Technol. 2(2). https://www.itu.int/dms_pub/itu-s/opb/jnl/S-JNL-VOL2.ISSUE2-2021-A02-PDF-E.pdf. Accessed September 23, 2023.

22 Wang L, Araniti G, Cao C, Wang W, Liu Y (2015) Device-to-Device users clustering based on physical and social characteristics. Int J of Distribu Sens Netw, 2015(165608):1-14. https://journals.sagepub.com/doi/pdf/10.1155/2015/165608. Accessed August 5, 2023.

23 Cao C, Wang L, Song M, Zhang Y (2014) Admission policy based clustering scheme for D2D underlay communications. *IEEE 25th Annu Int Symp on Pers, Indoor, and Mob Radio Commun (PIMRC)*, 1-6. DOI: 10.1109/PIMRC.2014.7136488

24 Zhou Y (2013) Performance evaluation of a weighted Clustering algorithm in NSPS scenarios (Thesis, Royal Institute of Technology (KTH), Stockholm, Sweden). http://www.diva-portal.org/smash/get/diva2:690435/FULLTEXT01.pdf Accessed September 18, 2013.

25 Imoize AL, Oseni AI (2019) Investigation and pathloss modeling of Fourth Generation Long Term Evolution Network along major highways in Lagos Nigeria. *Ife Jl of Sci*, *21*(1):39-60. https://dx.doi.org/10.4314/ijs.v21i1.4. Accessed July 23, 2023.

26 Balkorkian S, Zhang H (2005) Analysis of internal RF interferences in mobile phones (Master's thesis), Stockholm, Sweden. https://www.diva-portal.org/smash/get/diva2:9977/FULLTEXT01.pdf. Accessed June 6, 2023.

27 Scogna A, Shim H, Yu J, Oh C-Y, Cheon S, Oh N (2018) RFI and receiver sensitivity analysis in mobile electronic devices. *Signal Integrity Journal*, May 7, 2018. https://www.signalintegrityjournal.com/articles/843-rfi-and-receiver-sensitivity-analysis-in-mobile-electronic-devices. Accessed May 10, 2023.

28 Hwang C (2018) RF desensitization in wireless devices. In B. Mamun & A. Mohammad (Eds.), IntechOpen. 101-118. https://www.intechopen.com/chapter/pdf-download/60537/4536503. Accessed March 16, 2013.

29 Babun L (2015) Extended Coverage for Public Safety and Critical Communications Using Multi-hop and D2D Communications (Master's thesis). Florida International University Miami, Florida, USA. https://digitalcommons.fiu.edu/etd/1920. Accessed May 12, 2023.

30 Gadze JD, Agyekum KA, Nuagah SJ, Affum EA. (2019) Improved propagation models for LTE path loss prediction in urban & suburban Ghana. Int J of Wirel & Mob Netw (IJWMN), 11(6):35-53. https://arxiv.org/ftp/arxiv/papers/2001/2001.05227.pdf. Accessed May 10, 2023.

31 Anamuro CV, Varsier N, Schwoerer J, Lagrange X (2018) Simple modeling of energy consumption for D2D relay mechanism. Wirel Commun and Netw Conf Work, April 2018, Barcelone, Spain. https://hal-imt-atlantique.archives-ouvertes.fr/hal-01836546/file/Energy_consumption_D2D.pdf. Accessed June 2, 2023.

32 Rappaport TS (1996) Wireless communications: principles and practice. (Vol. 2). New Jersey: Prentice Hall PTR.

33 3GPP TR 36.843 v12.0.1 (2014b), "Study on LTE Device to Device Proximity Services," Release 12, March 2014. https://www.3gpp.org/ftp/Specs/archive/36_series/36.843/36843-c01.zip. Accessed August 13, 2023.

34 Lauridsen M, Noël L, Sørensen TB, Mogensen P (2014) An empirical LTE smartphone power model with a view to energy efficiency evolution. Int Technol J, 18(1):172-193. https://vbn.aau.dk/ws/portalfiles/portal/176790997/An_Empirical_LTE_Smartphone_Power_Model_with_a_View_to_Energy_Efficiency_Evolution.pdf. Accessed March 14, 2023.

35 Höyhtyä M. Apilo O, Lasanen M (2018) Review of latest advances in 3GPP standardization: D2D Communication in 5G systems and its energy consumption models. *Future Internet*, *10*(3):1-18. Doi:10.3390/fi10010003